VOL. 12, NO. 8, APRIL 2017 ISSN 1819-6608
ARPN Journal of Engineering and Applied Sciences

www.arpnjournals.com

COMPARATIVE STUDY ON ENERGY EXTRACTION FROM VIBRATING SQUARE CYLINDER

Nurshafinaz Mohd Maruai[1], Mohamed Sukri Mat Ali[1], Mohamad Hafiz Ismail[1], Sheikh Ahmad Zaki Shaikh Salim[1], Masataka Shirakashi[1] and Sallehuddin Muhamad[2]
[1]Wind Engineering Laboratory, Malaysia-Japan International Institute of Technology, Universiti Teknologi Malaysia, Malaysia
[2]Department of Engineering, UTM Razak School of Engineering and Advanced Technology, Universiti Teknologi Malaysia, Malaysia
E-Mail: nurshafinazmohdmaruai@yahoo.com

ABSTRACT

In this paper, the prospect of harvesting energy from flow induced-vibration of a square cylinder is assessed. The extraction of energy from the flow is attained by mounting the square cylinder on a one-degree elastic system with a mass-damping ($m^*\zeta$) of 2.75. OpenFOAM®, an open source CFD package is used to model the flow induced motion of the square cylinder. A theoretical formulation to estimate the lift force acting on the square cylinder is derived to confirm the results obtained by the simulation. A good agreement between the results is obtained. The amplitude vibration and lift force are then used to estimate the power induced by the oscillating square cylinder. Energy in the micro scale range can be harvested from this flow induced-vibration system. This type of alternative green energy is suitable for the micro energy harvester system required for sensors in many engineering structure for health monitoring purpose.

Keywords: square cylinder, flow-induced vibration, energy harvesting.

INTRODUCTION

The study of flow over bluff body and its influence towards flow induced vibration is certainly not new. Series of investigation from previous researchers has been acknowledged and well argued over past years [1][3][4][5]. Flow induced vibration has received much attention among researchers due to its close relationship with real case scenario such as the fallen Tacoma Narrow Bridge and many practical engineering structures' destruction. Hence, since over 60 years ago the main concern in this field is to reduce and suppress the vibration.

However, in these recent years the idea of utilizing this vibration driven by the presence of vortex shedding as the source for energy harvesting purpose has increased [16]in their study has introduced the state of art wind energy harvester from wake galloping phenomenon, which able to generate electricity sufficiently for commercial wireless sensor nodes(WSN) platform, IMote2[16].Another examples of investigations related to aeroelastic energy harvesting was conducted by[17-20].However, harvesting energy from the flow induced vibration using square cross section cylindrical bluff body is still not fully explored.

Square cylinder has fixed separation point making it susceptible to both vortex induced vibration (VIV) and galloping. VIV is an aerodynamic instability which may occur at relatively low onset velocity, while galloping may produce relatively high amplitude but occurs at later onset velocity. Thus, a wider access to both phenomena so to produce higher vibration amplitude at lower onset velocity is possible when using square cross section cylinder.

The current study will investigate the energy produced by the fluctuating force due to the occurrence of periodic vortex shedding in the wake of square cylinder.

The objectives of this study are to investigate:

i. The feasibility of flow induced vibration as the source of energy harvesting.
ii. The potential work done by the fluid force unto the cylinder
iii. The prediction of power produced by the vibration.

This manuscript is structured as follows and consists of 6 sections. Section 2 describes the problem geometry of a rigid square cylinder mounted on a one degree elastic system in free stream airflow. The fluid-structure modelling for numerical study is discussed in Section 3. This section elaborates the interaction of flow solver with the dynamic solver for flow field simulation. Section 4 describes the derivation of Single Degree of Freedom (1DOF) equation of motion to produce theoretical equation for lift in phase with velocity and energy transfer prediction. Results and discussion will be presented in Section 5. Finally, the conclusions of the study are presented in Section 6.

PROBLEM GEOMETRY

In this paper, we consider an incompressible airflow in free stream boundary condition around a square cylindrical bluff body with Reynolds Numbers, *Re*= 3536-8778. The square cylinder is mounted on a spring with stiffness k and damping coefficient c that is freely oscillating in a transverse direction to the incoming flow.

Following [9] the amplitude response of fluctuating displacement for cylindrical bluff body can be non-dimensionalized as

$$A^* = \frac{1}{4\pi^3}\frac{C_L \sin\Phi}{(m^* + C_A)\zeta}\left(\frac{U_R}{f^*}\right)^2 f^* \quad (1)$$

where A^* is the displacement of cylinder's motion y normalized by the side length of cylinder D, f^* is amplitude frequency normalized with natural frequency of the cylinder, $C_L$is the lift coefficient, Φ is the phase delay between the signals of fluid force and cylinder's motion, m^* is the mass ratio and $C_A$is added mass coefficient assumed to be C_A=1 in current study.

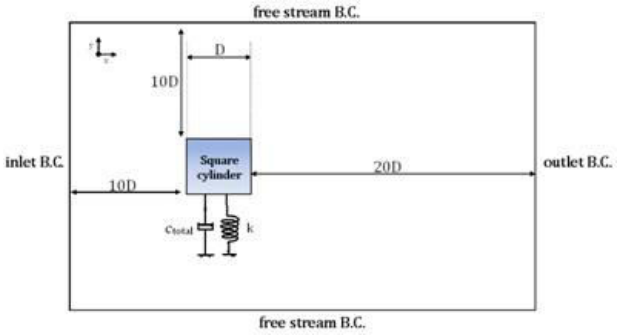

Figure-1. Sketch of problem geometry.

Figure-1 shows the schematic diagram of problem geometry with fixed free stream reduced velocity U_R at the inlet situated 10Dupstream of the square cylinder. The upper and lower walls are considered free stream boundary with no slip boundary condition. The physical parameters are presented in Table-1.

Table-1. Physical parameters.

Parameter	Magnitude
Square cylinder side length, D[m]	0.026
Logarithmic damping factor, δ	0.0275
Total damping factor, ζ	0.004377
Spring stiffness, k[N/m]	1173.05
Mass damping ratio, m* ζ	2.75

FLUID-STRUCTURE MODELLING

Flow solver

The flow is modelled according to the conversion law of mass and momentum in predefined volume. The flow solutions are obtained by solving the Unsteady Reynolds Averanged Navier-Stokes (URANS) equations. Consider the flow is incompressible, the continuity and incompressible Navier-Stokes equations are given as follow:

$$\frac{\partial u_i}{\partial x_i} = 0 \tag{2}$$

$$\rho\frac{\partial \bar{u}_i}{\partial t} + \rho\bar{u}_j\frac{\partial \bar{u}_i}{\partial x_j} = \frac{\partial}{\partial x_j}\left[-\bar{p}\delta_{ij} + \mu\left(\frac{\partial \bar{u}_i}{\partial x_j} + \frac{\partial \bar{u}_j}{\partial x_j}\right) - \rho\overline{u'_i u'_j}\right] \tag{3}$$

Here $\bar{u}$ is the time averaged velocity while $\tau_{ij} = -\rho\overline{u'_i u'_j}$denotes the Reynolds stress tensor. Reynolds stress tensor is a turbulence transport term, which implies the fluctuating velocities to the total change in conservation of momentum. Subscripts i and j represent the tensor index notation of two dimensional Cartesian coordinate. The Reynolds stress tensor is solved using the Boussinesq assumption

$$\tau_{ij} = -\rho\overline{u'_i u'_j} = \mu_t\left(\frac{\partial u_i}{\partial x_j} + \frac{\partial u_j}{\partial x_i} - \frac{2}{3}\frac{\partial u_k}{\partial x_k}\right) - \frac{2}{3}\rho k\delta_{ij} \tag{4}$$

In present case we employed the SST k-ω turbulence model with addition of two transport equations in order to determine the Reynolds stress tensor and simultaneously solve the governing equations [10].The turbulence properties of the flow, namely turbulent kinetic energy k and turbulent dissipation rate ω are represented in following equations:

Turbulent kinetic energy k

$$\frac{\partial \rho k}{\partial t} + u_j\frac{\partial(\rho k)}{\partial x_j} = \tau_{ij}\frac{\partial u_i}{\partial x_j} - \beta^*\rho\omega k + \frac{\partial}{\partial x_j}\left[(\mu + \sigma_k\mu_k)\frac{\partial k}{\partial x_j}\right] \tag{5}$$

Turbulent dissipation rate ω

$$\frac{\partial \rho\omega}{\partial t} + u_j\frac{\partial(\rho\omega)}{\partial x_j} = \tau_{ij}\frac{\gamma}{\nu_t} - \beta\rho\omega^2 k \ldots + \frac{\partial}{\partial x_j}\left[(\mu + \alpha_\omega\mu_t)\frac{\partial \omega}{\partial x_j}\right] \ldots + 2\rho(1-F_1)\sigma_{\omega 2}\frac{1}{\omega}\frac{\partial k}{\partial x_i}\frac{\partial \omega}{\partial x_j} \tag{6}$$

Dynamic solver

An oscillating model in Figure-2 is deployed and its dynamic response due to fluid force based on the equation of motion for oscillating cylinder following [13] is presented by a second order of linear equation:

$$m_e\ddot{Y} + c\dot{Y} + kY = Lift \tag{7}$$

Here m_e is the total mass of oscillating cylinder, k is the spring stiffness and c is the total damping coefficient for oscillating cylinder. Lift in this study is considered constant in a small time step, Δt.

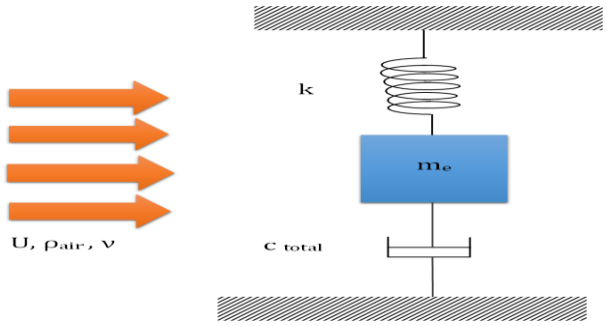

Figure-2. Model of oscillating cylinder.

In order to preserve the precision of the solution, the mesh around cylinder is permitted to deform accordingly to the Laplace smoothing equation.

$$\nabla.(\gamma \nabla u) = 0 \tag{8}$$

Here u is the mesh deformation velocity of the mesh and $\gamma$is displacement diffusion. The mesh deformation velocity will renew the point's position of mesh distribution;

$$x_{new} = x_{old} + u\Delta t \tag{9}$$

and simultaneously solve the Equation. (2) and Equation. (3).

ENERGY TRANSFER MODELLING

The prediction of energy transfer between the fluid forcing and flexible rigid body has yet to be confirmed. One of the means to predict the behaviour of FIV is by considering the power in the fluid using the Bernoulli principle for dynamic pressure. However, this formulation only limited for the flow along the streamline in the core region and not applicable to flow nears the surface. There is another approach to predict the energy transfer that is by implying the calculation for lift in phase with velocity suggested by previous researchers.

The theoretical formula

In this section author would like to derive a formula to estimate lift force acting on the square cylinder. The formulation is based on the approach suggested by Parkinson.

Lift in phase, $C_y \sin \Phi$

The study of energy transfer between the flow and the oscillating body or the work done unto the body due to the occurrence of alternating vortex shedding force is obtainable by first deriving the conventional first degree freedom (1DOF) equation of motion in Equation.(10)[5].

$$m\ddot{y} + c_{total}\dot{y} + ky = F_y(t) \tag{10}$$

Here y is the displacement of cylinder's motion transverse to the incoming flow while $\ddot{y}$ and $\dot{y}$ are the acceleration and velocity of the body motion in y-axis respectively. The properties of an elastic rigid body are represented by the terms, namely mass m, structural damping c and spring stiffness k.

$$y(t) = y_0 \sin(\omega t) \tag{11}$$

Here, $y_0$is the maximum displacement of cylinder's motion. Following [5] fluid force is described as

$$F_y(t) = \frac{1}{2}\rho U^2 D L c_y(t) \tag{12}$$

The left hand side equation is first decomposed by replacing the $\ddot{y}$ and $\dot{y}$ terms into its derivation result in y term.

$$\ddot{y} = -\omega^2 y_0 \sin(\omega t) \tag{13}$$

$$\dot{y} = \omega y_0 \cos(\omega t) \tag{14}$$

$$(k - m\omega^2 y_0)\sin(\omega t) + c\omega y_0 \cos(\omega t) = F_y(t) \tag{15}$$

The only non –zero energy term is the term, which in phase with velocity $\dot{y}$[6]. Therefore, it is preserved to be included in the next step. Due to some arrangement and replacement, the velocity term is written as below

$$2\zeta m\omega_n \omega y_0 \cos(\omega t) = F_y(t) \tag{16}$$

Here the damping term is replaced with $c_{total} = 2\zeta\sqrt{km} = 2\zeta m\omega_n$,when$\omega_n = \sqrt{\frac{k}{m}}$.

Due to [4]the lift coefficient is divided into two components. One is corresponding with the acceleration term due to the added mass, while the other is corresponding to the velocity term, which signifies the energy transfer behaviour. The decomposition of the lift coefficient is described as follows

$$c_y(t) = C_y \sin(\omega t + \Phi)$$

$$= C_y \sin(\omega t)\cos\Phi + C_y \sin\Phi \cos(\omega t) \tag{17}$$

Here Φ is the phase delay between the signals from fluid force, F_y(t) and cylinder motion, y(t). It indicates the direction of energy transfer between the flow and oscillating body. Since the energy transfer is only valid when the phase shift, $0°<\Phi<180°$ the acceleration term nonresponsive to the validity condition is cancelled out and left with

$$c_y(t) = C_y \sin\Phi \cos(\omega t) \tag{18}$$

The left and right hand side equations are combined and written in Equation. (16) below

$$2\zeta m\omega_n \omega y_0 \cos(\omega t) = \frac{1}{2}\rho U^2 DLC_y \sin\Phi \cos(\omega t) \quad (19)$$

Next the equation is rearranged and written as the lift coefficient in phase with the cylinder motion as one of the important component for energy transfer.

$$C_y \sin\Phi = 8\pi^2 \frac{y_0}{D}\left(\frac{2m\zeta}{\rho D^2}\right)\left(\frac{f_n D}{U}\right)^2 \frac{1}{L}\frac{f}{f_n} \quad (20)$$

Here the equation is simplified into

$$C_y \sin\Phi = \frac{y_0}{D} 8\pi^2 \frac{Sc}{{U_R}^2}\frac{1}{L}\frac{f}{f_n} \quad (21)$$

where Sc is Scruton number and U_R is reduced velocity. This equation shows good agreement with the calculation done by [5]for three dimensional bodies.

Energy transfer between flow field and oscillating body

In this subsection the work done on the body and the exerted power under FIV condition is derived and conceptualized. A conceptual sketch for power conversion of oscillating cylinder is shown in Figure-3 and will be assessed to predict the induced power from cylinder's oscillation due to the fluid force. The work done unto the body is described as the integration product of fluid force, $F_y(t)$ and velocity term of body motion in T cycle oscillation [6]

$$W = \int_0^T F_y(t).\dot{y}\,(t) \quad (22)$$

The result of the above integration is

$$W = \frac{\pi}{2} y_0 C_y \sin\Phi \rho U^2 \mathrm{DL} \quad (23)$$

Whereas the power of fluid exerted to the body is determined by averaging the work done with T cycle of oscillation.

$$P = \frac{W}{T} \quad (24)$$

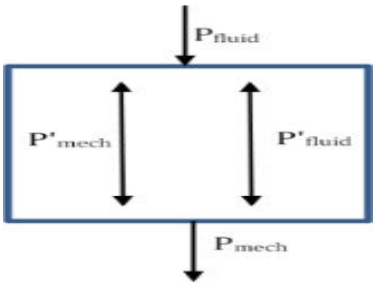

Figure-3. Conceptual sketch for power conversion of oscillating square cylinder.

During lock-in synchronization we find that oscillation frequency is equal to the frequency of vortex shedding and simultaneously is equal to the frequency in a cycle. Therefore T in the equation can also be described as $\frac{1}{f}$and the equation written as

$$P'_{fluid} = \frac{\pi}{2} y_0 f C_y \sin\Phi \rho U^2 \mathrm{DL} \quad (25)$$

These equations are utilized to predict the behaviour of energy transfer from the fluid force towards the cylinder and the results will be discussed in Section5.

RESULTS AND DISCUSSIONS

Amplitude response

Figure-4(a) shows the RMS value of body motion's displacement transverse to the incoming flow of the current numerical study. Experimental measurements using the same facility and method as Kawabata [5] are plotted for comparison. Additionally, experimental investigation for the similar study by Kawabata [5] is also plotted.

Current numerical results predict well with VIV response. The second peak of amplitude response occurred due to the rotational motion from spanwise instability. The lower branch velocity shows the VIV behaviour with a sudden rise at after U_R = 15, which signifies a galloping behaviour.

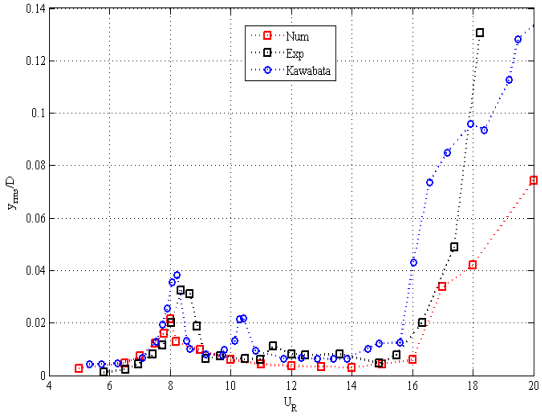

Figure-4a). Root mean square transverse amplitude with reduced velocity (red-numerical, black –experimental, blue- Kawabata [12]).

The data series of maximum amplitude are also plotted as it will be used to calculate the lift, work and power prediction using theoretical equation. Both numerical and experimental show good agreement and presented in Figure-4(b).

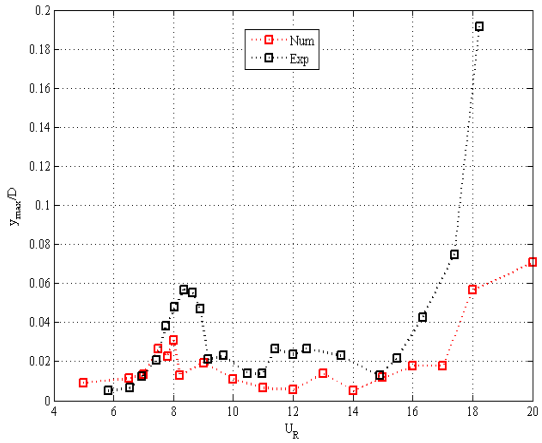

Figure-4b). Maximum transverse amplitude with reduced velocity (red-numerical, black –experimental).

Frequency response

The dominant oscillation frequency *f*is retrieved by processing the displacement time histories using the Fast Fourier Transform (FFT) equation to assure the frequency matching condition is preserved and correctly determined. The solutions were plotted in Figure-5.

Power Spectrum Density analysis for both vibration and vortex shedding behaviour shows a VIV response at lower frequency and predict well with the experimental study result. The lock-in synchronization is shown once again at higher frequency regime as U_R continues to increase with a sudden drop at U_R = 15, which indicates the starting point for galloping behavior

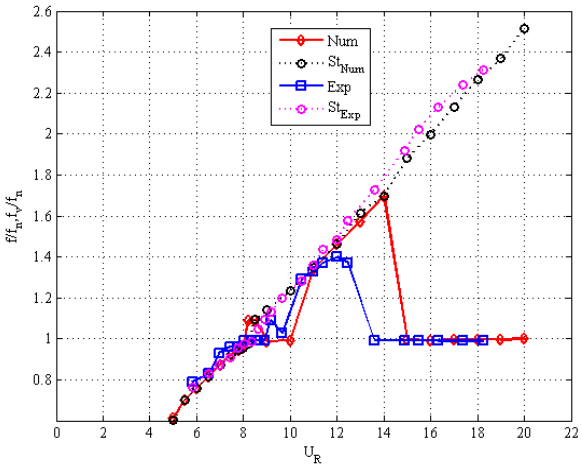

Figure-5. Comparison of frequency responses between numerical and experimental study.

Lift, work and power of oscillating cylinder

Lift in phase, C_y sin Φ

The data collection of lift force is not measuredduring experimental studies. Due to this deficiency author has determined to investigate this concern and find alternative solution to assess the magnitude of lift coefficient from existing data. Parkinson in his previous study has suggested a formula which consistent with Equation. (20).

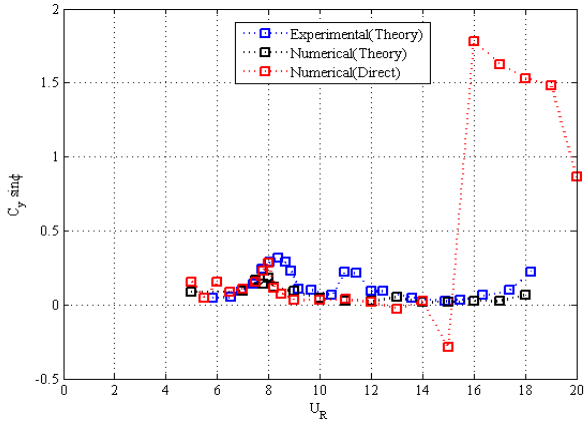

Figure-6. Comparison of lift in phase with cylinder's velocity motion between numerical data and experimental prediction (red – numerical data, black – numerical prediction, blue –experimental prediction).

Figure-6 shows the comparison of lift in phase with velocity between direct computation value from numerical study and by means of theoretical equation. The graph pattern and magnitude are comparable for lower velocity branch. While, the pattern of lift in phase with velocity for direct computation and prediction are contradict for higher velocity branch. This is due to the assumption made in the earlier derivation of formula where the lift is assumed in phase with the amplitude vibration. However in the galloping region, the lift and the amplitude is not in phase.

Work, W

The findings for lift in phase were then used to evaluate the work done unto the cylinder to cause in oscillation. The graph was plotted in Figure-7 based on the Equation. (23).

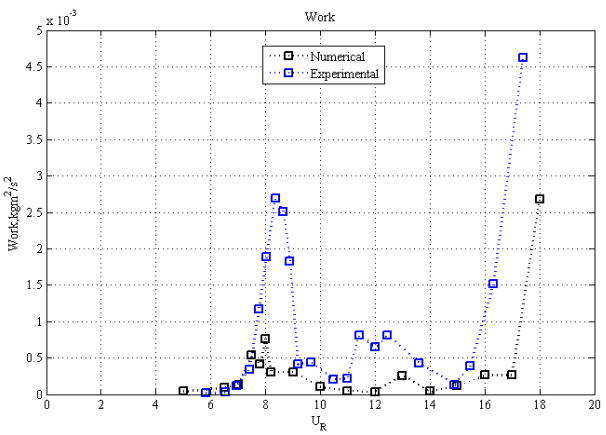

Figure-7. Comparison between numerical prediction and experimental prediction for work done on the cylinder.

Power on the cylinder,P'_{fluid}

Finally based on the lift in phase computed as in Equation. (20), the power prediction is determined using Equation. (25) and the graph is plotted in Figure-8.

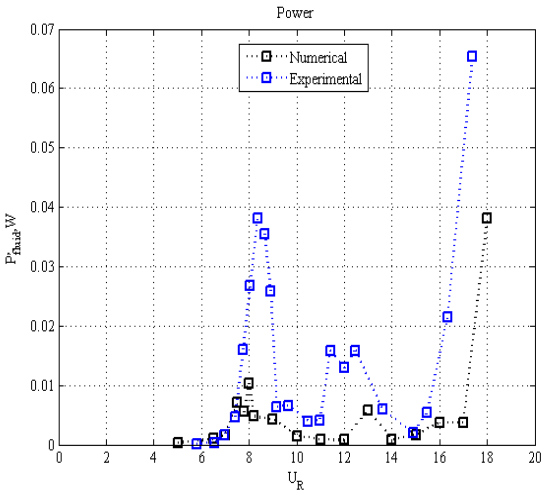

Figure-8. Comparison between numerical prediction and experimental prediction for power exerted towards the cylinder.

CONCLUSIONS

The flow around a square cylinder, which elastically mounted with spring stiffness k and damping c_{total} was numerically investigated and compared with prior experimental measurements. The findings show two significant flow induced vibration's behaviours, namely vortex-induced vibration and galloping. The VIV occurred at the lower branch velocity while galloping starts at higher branch velocity (U_R=15). The galloping behaviour was confirmed by the frequency response with a sudden drop of its vibration frequency at mentioned velocity. An equation for lift in phase with velocity was arithmetically derived and confirmed with the lift obtained by numerical simulation. The solution to the equation was plotted and shows a good agreement between numerical and experimental study at lower branch velocity, which indicates the regime for VIV behaviour.

ACKNOWLEDGEMENTS

This research was financially supported by Malaysia Ministry of Higher Education (MOHE) under Research University Grant (RUG) project of Universiti Teknologi Malaysia (Vot No. Q.K130000.2643.09J79) and (Vot No. R.K130000.7843.4F479) also High Performance Computer (HPC) Universiti Teknologi Malaysia for the use of their supercomputer facilities. The first author also would like to acknowledge Universiti Teknologi Malaysia for the receipt of Ph.D scholarship.

REFERENCES

[1] Blevins R. D. 1990. Vibration of structures induced by fluid flow. Harris' Shock and Vibration Handbook. pp. 19.

[2] Davenport A. G. and Novak M. 1976. Vibration of structures induced by wind. Shock and vibration handbook. (Part II). pp. 29-21.

[3] Williamson C. H. K.and Govardhan R. 2004. Vortex-induced vibrations. Annu. Rev. Fluid Mech. 36. pp. 413-455.

[4] Sarpkaya T. 1979. Vortex-induced oscillations: a selective review. Journal of Applied Mechanics. 46(2). pp. 241-258.

[5] Parkinson G. 1989. Phenomena and modelling of flow-induced vibrations of bluff bodies. Progress in Aerospace Sciences. 26(2). pp. 169-224.

[6] Bernitsas M. M., Raghavan K., Ben-Simon Y., and Garcia E. M. 2008. VIVACE (Vortex Induced Vibration Aquatic Clean Energy): A new concept in generation of clean and renewable energy from fluid flow. Journal of Offshore Mechanics and Arctic Engineering. 130(4). pp. 041101.

[7] Ding L., Zhang L., Wu C., Mao X., and Jiang D. 2015. Flow induced motion and energy harvesting of bluff bodies with different cross sections. Energy Conversion and Management. 91. pp. 416-426.

[8] Koide M., Sekizaki T., Yamada S., Takahashi T., and Shirakashi, M. 2013. Prospect of Micro Power Generation Utilizing VIV in Small Stream Based on Verification Experiments of Power Generation in Water Tunnel. Journal of Fluid Science and Technology. 8(3). pp. 294-308.

[9] Khalak A., and Williamson C. H. K. 1999. Motions, forces and mode transitions in vortex-induced vibrations at low mass-damping. Journal of fluids and Structures. 13(7). pp. 813-851.

[10] Menter F. R. 1994. Two-equation eddy-viscosity turbulence models for engineering applications. AIAA journal. 32(8). pp. 1598-1605.

[11] Barrero-Gil A., and Fernandez-Arroyo P. 2013. Maximum vortex-induced vibrations of a square prism. Wind and Structures. 16(4). pp. 341-354.

[12] Kawabata Y., Takahashi T., Haginoya T., and Shirakashi, M. 2013. Interference Effect of Downstream Strip-Plate on the Crossflow Vibration of a Square Cylinder. Journal of Fluid Science and Technology. 8(3). pp. 348-363.

[13] Guilmineau E., and Queutey P. 2004. Numerical simulation of vortex-induced vibration of a circular cylinder with low mass-damping in a turbulent flow. Journal of fluids and structures. 19(4). pp. 449-466.

[14] Durfee, W., and Sun Z. 2009. Fluid power system dynamics. Center for Compact and Efficient Fluid Power.

[15] Billah K. Y., and Scanlan R. H. 1991. Resonance, Tacoma Narrows bridge failure, and undergraduate physics textbooks. Am. J. Phys. 59(2). pp. 118-124.

[16] Jung H. J., Lee S. W., and Jang D. D. 2009. Feasibility study on a new energy harvesting electromagnetic device using aerodynamic instability. Magnetics, IEEE Transactions on. 45(10). pp. 4376-4379.

[17] Li S., Yuan J., and Lipson H. 2011. Ambient wind energy harvesting using cross-flow fluttering. Journal of Applied Physics. 109(2). pp. 026104.

[18] Abdelkefi A., Hajj M. R., and Nayfeh A. H. 2012. Power harvesting from transverse galloping of square cylinder. Nonlinear Dynamics. 70(2). pp. 1355-1363.

[19] Weinstein L. A., Cacan M. R., So P. M., and Wright P. K. 2012. Vortex shedding induced energy harvesting from piezoelectric materials in heating, ventilation and air conditioning flows. Smart Materials and Structures. 21(4). pp. 045003.

[20] Park J., Morgenthal G., Kim K., Kwon S. D., and Law K. H. 2014. Power evaluation of flutter-based electromagnetic energy harvesters using computational fluid dynamics simulations. Journal of Intelligent Material Systems and Structures. 1045389X14526954.